

Transport of Current by Whistler Waves

J. M. Urrutia and R. L. Stenzel

Department of Physics, University of California at Los Angeles, Los Angeles, California 90024-1547

(Received 28 June 1988)

When an electrode is immersed in a laboratory plasma with magnetized electrons and its bias is pulsed with respect to the plasma potential so as to collect either ions or electrons, the initial current in the plasma is always carried by electrons. The dc current front is preceded by oscillatory dispersive currents which, for our experimental conditions, are associated with whistler waves. Thus, the current front advances along \mathbf{B}_0 not at particle speeds but at the whistler wave speed.

PACS numbers: 52.25.Fi, 52.35.Hr, 52.40.Db, 52.40.Hf

The steady-state concept¹ that currents between electrodes immersed in plasmas are carried by the species collected across the electrode sheath (electrons when the electrode is biased positive, ions when it is biased negative with respect to the plasma potential) is often applied to time-dependent situations. For example, in the steady state, charged particles are thought to drift into the electrode with their random thermal velocity; hence one may (mistakenly) assume that upon turn on of a positive or negative voltage to an electrode the current penetrates at $v_e = (kT_e/m_e)^{1/2}$ or $v_i = c_s = (kT_e/m_i)^{1/2}$, respectively. Laboratory² and computer³ experiments on time-dependent currents have been performed; however, the steady state is assumed to have been reached once the sheath is established (typically, several plasma periods). As stated elsewhere,³ these assumptions form the basis of many current systems studied in the laboratory and space (e.g., diagnostic probes, antenna response, beam emission, etc.). In this Letter we report *in situ* measurements of the magnetic-field perturbations caused by switching currents to cold electrodes in a magnetized afterglow plasma (magnetized electrons and weakly magnetized ions). Because of the respective magnetization as well as due to weak collisionality ($v_{ei}/\omega_{ce} \ll 1$), electron currents are theoretically confined to the flux tube subtended by the electrode while ion currents are not. Instead, our observations of current flow and propagation speed indicate that for both positive and negative electrodes, the initial current is dominated by electrons and associated electromagnetic waves and therefore flows almost exclusively along the externally imposed magnetic field. However, once dc currents are established, cross-field transport of current is evident. The spread appears to be due to self-consistent electric fields and the geometry of the volume over which current flows.⁴ Space- and time-resolved measurements reveal a new observation: The current front contains induced reverse currents (consistent with Lenz's law) which are oscillatory dispersive structures propagating at the whistler wave speed (consistent with the collective electron mode which convects magnetic-field perturbations in magnetoplasmas).⁵

The experiments are conducted in the quiescent afterglow ($t \approx 120 \mu\text{s}$) of a large linear (1 m diam, 2 m length) pulsed ($t_{\text{rep}} \approx 2 \text{ s}$, $t_{\text{on}} \approx 4 \text{ ms}$) magnetoplasma ($n_e \approx 8 \times 10^{11} \text{ cm}^{-3}$, $kT_e \approx 5kT_i \approx 1.0 \text{ eV}$, $B_0 = 5\text{--}30 \text{ G}$, $P_{\text{Ar}} = 0.4 \text{ mTorr}$) schematically shown in Fig. 1(a). The electrodes are tantalum or copper disks of various diameters (2–66 cm). The chamber wall and grounded grid anode serve as the return electrode. The biasing circuit is pulsed with a typical rise time of 30 ns ($2\pi/\omega_{ci} \approx 2.6 \text{ ms} > t \approx 2\pi/\omega_{ce} \approx 35 \text{ ns}$ at 10 G). The magnetic field, $\mathbf{B}(\mathbf{r}, t)$, induced by the current flow is measured with a probe consisting of three electrostatically shielded, small (1 cm diam), orthogonal magnetic loops. The probe tip is capable of scanning a suitably large volume ($0 < r < 20 \text{ cm}$, $0 < z < 55 \text{ cm}$) about the electrode. Thus, complete maps of the total current density ($\mathbf{J} = \mathbf{J}_{\text{cond}} + \partial\mathbf{D}/\partial t = \nabla \times \mathbf{H}$) in the plasma are available⁴

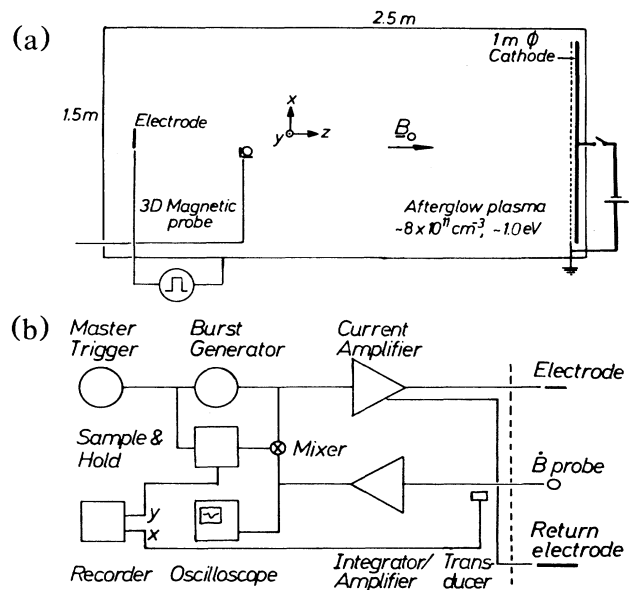


FIG. 1. (a) Schematic diagram of the experimental device. (b) Block diagram of the data processing system.

although the experiments reported here do not require them on account of cylindrical symmetry. Wave information is obtained with a gated interferometer circuit consisting of various integrators and amplifiers, a mixer, a tone burst generator, and a sample-and-hold unit [Fig. 1(b)].

First, a disk electrode ($r=10$ cm, surface normal is along $\mathbf{B}_0=30$ G) is biased so as to collect electrons ($I_{e,\max}=2$ A). Figure 2 displays $B_\theta(t)$ (in arbitrary units, field magnitude is on the order of a few mG) at various axial distances, z , from the electrode at $r=20$ cm, $\theta=0$. Because of the system's cylindrical symmetry ($\partial/\partial\theta=0$), the axial current density is given by $\mu_0 J_z = 1/r \partial(rB_\theta)/\partial r$. After the initial transient (discussed below), the quasi-steady-state [$t \geq 20 \mu\text{s}$, Fig. 2(b)] value of B_θ decreases with z . Since it does so at all radial positions (not shown), J_z decreases with increasing axial distance. The current must then flow across \mathbf{B}_0 ($\nabla \cdot \mathbf{J}=0$) and the surface through which it flows is therefore a cone with base at the electrode instead of the end walls of the theoretical magnetic flux tube. Consequently, cross-field transport of electrons takes place. Given our parameter range ($n_e \approx 8 \times 10^{11}$, $B_0=30$ G, $kT_e \approx 1$ eV), classical conductivity ($\sigma_\perp/\sigma_\parallel \approx (v_{ei}/\omega_{ce})^2 \approx 0.002$) does not account for the decrease in J_z . However, if self-consistent electric fields are present (given by $\mathbf{J}=\sigma \cdot \mathbf{E}$, where σ , the conductivity tensor, contains *all* off-diagonal terms which allows for \mathbf{E}_\perp to be a function of \mathbf{J}_z), then the transport can be understood.⁴ Measurement of such fields is outside the scope of this Letter.

Most interesting is the transient response of the plasma to the turn on and turn off of the external current I_e . Figure 2 shows the evolution of a dispersive oscillation in $B_\theta(z,t)$ which, incidentally, also appears in $B_z(z,t)$ (not shown). This indicates that a current loop is induced as a result of the change in magnetic flux in the electrode's vicinity due to the electron collection. In addition to the inductive electric fields responsible for the current loop, the particle collection must also give rise self-consistently to a space-charge field since neutralizing electrons take time to travel to the electrode. Because the perturbed magnetic field can penetrate into the plasma at a finite speed determined by the plasma dispersive properties, the induced current loop cannot close at the distant return electrode but must do so locally. As expected from Lenz's law, other loops, of appropriate direction and magnitude, form downstream [Fig. 2(b)]. Thus the oscillatory current propagates away from the electrode similarly to electromagnetic waves emitted by an antenna. In fact, it exhibits the characteristics of a whistler wave as established in detail below. Because of the frequency dependency of the phase and group velocities of whistlers, the various maxima and minima shown in Fig. 2(a) travel at different speeds [(0.5–2.5) $\times 10^7$ cm/s] and the dc current rise spreads in time. Such transient waveforms would not be observed if the current propagated at speeds solely determined by the electron

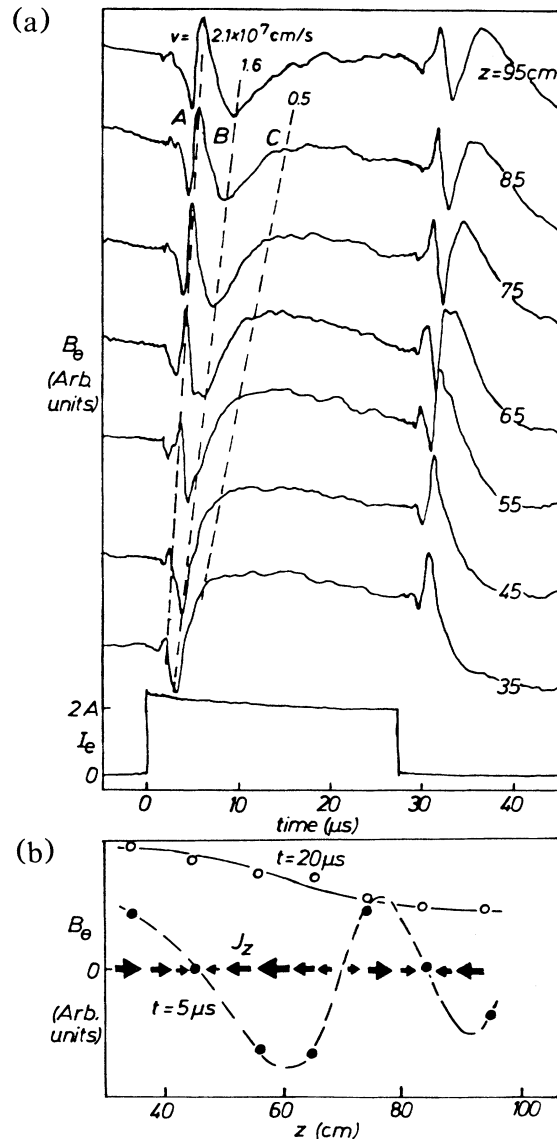


FIG. 2. (a) Externally measured electron current, $I_e(t)$ (lower trace, $I_{e,\max}=2$ A) and the internal perturbed magnetic field B_θ vs time (in arbitrary units) at different distances z from the electrode along the axial dc magnetic field, \mathbf{B}_0 . The different speeds of the maxima and minima (dashed lines A and B), as well as that of the dc current front (dashed line C), result from the dispersion of whistler waves [$v \approx 10^7$ cm/s, decreasing velocity with decreasing frequency, see Fig. 4(c)]. (b) For a given time after current turn on (e.g., $t = 5 \mu\text{s}$), the magnetic field in the plasma oscillates spatially indicating that the induced field is wavelike and that current loops are established (schematically indicated by arrows in figure center). After establishment of dc current (e.g., $t = 20 \mu\text{s}$), the magnetic field decreases axially indicating current spread (see text).

thermal velocity. Another induced current system is formed after the current pulse is terminated. In this case, since the magnetic flux decreases, the plasma at-

tempts to sustain the dc field. Again, as a result of local closure, other loops develop downstream and propagate with speeds similar to those observed during the turn-on phase. The source of energy driving these fields is the magnetic energy stored in the plasma during dc current flow.

As mentioned above, ion collection is assumed to give rise to currents carried by weakly magnetized ions propagating at any angle with respect to \mathbf{B}_0 at the ion sound speed ($c_s \approx 2 \times 10^5$ cm/s). Figure 3 shows that these postulates are not borne out even when large ion currents are collected ($I_i \approx 20$ A, $r_{\text{disk}} = 66$ cm). We observe, as in the case of electron collection, the formation of an induced wavelike system and its propagation into the plasma at whistler wave speeds ($v_w \gg c_s$) mostly along the ambient magnetic field. While there is no doubt that ions are collected through the electrode's sheath, the data nevertheless indicate that electrons repelled from the electrode region carry the current in the plasma. If the current was carried by ions then the arrival time of the current front would be $t = z/c_s \approx 200$ μ s (at $z = 40$) instead of $t \approx 4$ μ s as in Fig. 3.

Since induced current oscillations are generated at switch on and switch off, it is natural to apply a rapidly switched current in order to resonantly drive whistler currents. With the setup of Fig. 1(b) a current tone burst ($I_e \approx 1$ A, 50% duty cycle) is applied and the phase-coherent B fields measured interferometrically along the axis of the electrode's flux tube. First, we determine the phase velocity of the waves along the ambient magnetic field, \mathbf{B}_0 , by introducing delay lines in the signal path of the interferometer. Figure 4(a) reveals

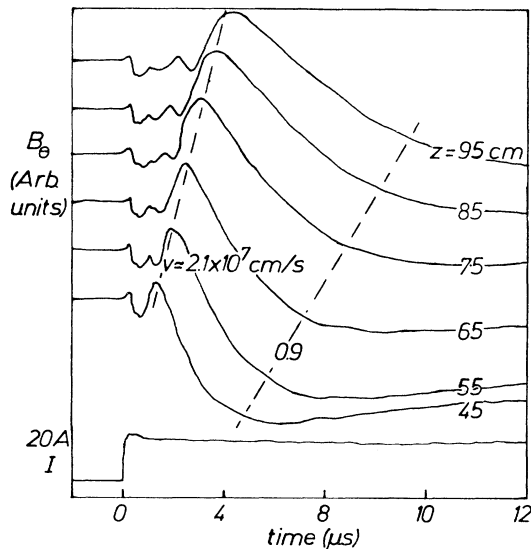


FIG. 3. Magnetic field $B_0(t)$ (in arbitrary units) measured along a line as in Fig. 2(a) but for the case of ion collection ($I_{i,\text{max}} = 20$ A, lower trace). Propagation speed indicates that in the plasma volume the current is carried by electrons.

that the weakly damped wave travels away from the electrode. Note that the phase velocity ($v_\phi \approx 2 \times 10^7$ cm/s) is below the electron thermal velocity ($v_{\text{th},e} \approx 6 \times 10^7$ cm/s). Next we examine the wave polarization by recording the transverse field components, B_x and B_y [Fig. 4(b)]. A 90° phase lag between B_x and B_y , characteristic of right-hand circular polarization, is observed. The third component, B_z (not shown), also displays an oscillation but lags B_x by 180° . This confirms that the oscillatory current forms spatially lo-

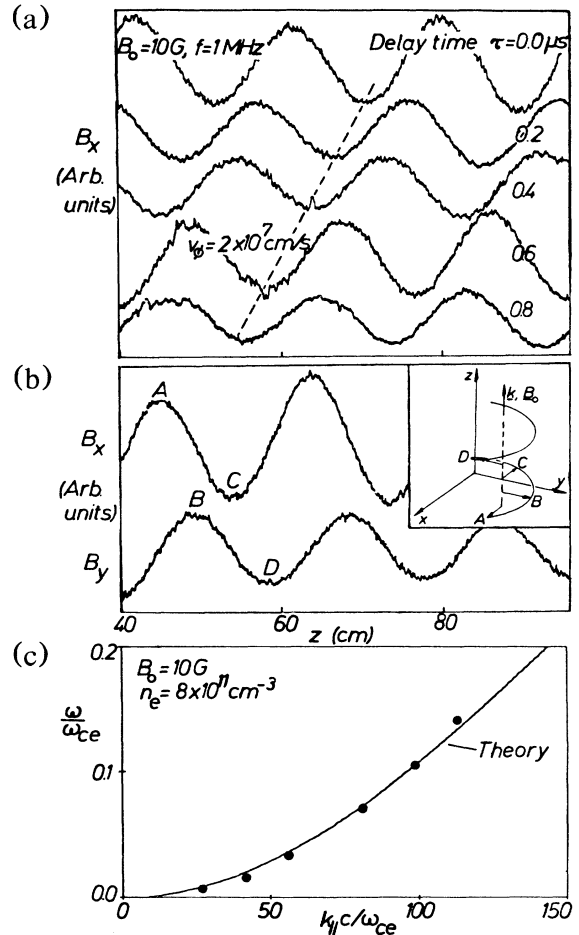


FIG. 4 (a) Interferometer traces B_x vs z for various delay times, τ , introduced into the signal leg [see Fig. 1(b)]. B_x is induced by a pulsed electron current ($I_e = 1$ A, $\omega/2\pi = 1$ MHz, 50% duty cycle). The motion of the phase fronts indicates that weakly damped waves move away from the electrode at whistler wave speeds ($v_\phi \approx 2 \times 10^7$ cm/s). (b) Polarization of $\mathbf{B}_{\text{wave}}(z) = [B_x(z), B_y(z)]$. As the axial distance from the electrode is increased the magnetic field rotates from B_x into B_y indicating right-hand circular polarization characteristic of whistler waves (see inset). (c) Measured dispersion relation, ω/ω_{ce} vs $k_{\parallel}c/\omega_{ce}$ (dots), of the perturbed magnetic field associated with periodically pulsed electron currents. The solid line is the theoretical dispersion relation for whistler waves, $c^2 k_{\parallel}^2 / \omega^2 = 1 - (\omega_{pe}^2 / \omega^2) (1 - \omega_{ce} / \omega)^{-1}$.

calized loops as deduced from Fig. 2. Finally we obtain the dispersion relation of the waves by varying the toneburst frequency and measuring the axial wave number k_{\parallel} for different values of $|\mathbf{B}_0|$ and n_e . Figure 4(c) displays one set of such measurements which shows excellent agreement between the data and the theoretical whistler dispersion relation for longitudinal propagation⁵

$$\frac{c^2 k_{\parallel}^2}{\omega^2} = 1 - \frac{\omega_{pe}^2/\omega^2}{1 - \omega_{ce}/\omega}.$$

Use of plane-wave, infinite-medium theory is justified since $v/\omega_{ce} \ll 1$ and $\omega_{pe} r_{\text{plasma}}/c \gg 1$.⁶

From the experimental observations reported in this Letter we can draw three interesting conclusions.

(1) Field-aligned switched currents to electrodes are dominated by the electron dynamics even if the electrode draws ions from the plasma. The momentum transfer is thought to occur in the sheath. These results hold even for electrodes larger than the ion Larmor radius.

(2) The penetration of currents into plasmas occurs neither at the Alfvén speed (MHD concept) nor at the electron thermal velocity (single-particle concept) but at the whistler wave speed (collective electron mode).

(3) A step function in the externally applied current waveform evolves in the plasma as an oscillatory dispersive wave train of falling frequencies in time, asymptotically approaching the dc current. The wave packet propagates with little damping within the whistler wave ray cone along \mathbf{B}_0 ($\theta_{\text{min}} \approx 11^\circ$ at $\omega/\omega_{ce} \approx 0.19$).⁵

If the electrode were moving across \mathbf{B}_0 then the dc current would flow along a winglike structure, a topic extensively discussed for satellite applications.⁷ Note, however, that our observations would predict whistler wings rather than the commonly assumed Alfvén wings. Pulsed currents are clearly suited to excite whistler

waves; beams are not better exciters since the associated current does not propagate at the beam speed⁸ but at the whistler speed. The present results are also important to the dynamics of neutral sheets in laboratory⁹ and space plasmas.¹⁰ The coupling of whistler waves to currents is also of interest to rf current drive in magnetic confinement devices.¹¹

The research was supported by NSF Grants No. PHY87-13829 and No. ATM87-02793.

¹H. M. Mott-Smith and I. Langmuir, *Phys. Rev.* **28**, 724 (1926); F. F. Chen, in *Plasma Diagnostic Techniques*, edited by R. H. Huddleston and S. Leonard (Academic, New York, 1965), Chap. 4; I. H. Hutchinson, *Principles of Plasma Diagnostics* (Cambridge Univ. Press, Cambridge, 1987).

²J. F. Weymouth, *J. Appl. Phys.* **30**, 1404 (1959).

³J. E. Borovsky, *Phys. Fluids* **31**, 1074 (1988).

⁴J. M. Urrutia, Ph.D. thesis, University of California at Los Angeles, Center for Plasma Physics and Fusion Engineering Report No. PPG 1115, October, 1987 (unpublished).

⁵R. A. Helliwell, *Whistlers and Related Ionospheric Phenomena* (Stanford Univ. Press, Stanford, 1965).

⁶J. P. Klozenberg, B. McNamara, and P. C. Thonemann, *J. Fluid Mech.* **21**, 545 (1965).

⁷C. E. Rassmussen, P. M. Banks, and K. J. Harker, *J. Geophys. Res.* **90**, 505 (1985), and references therein.

⁸R. L. Stenzel and J. M. Urrutia, *Geophys. Res. Lett.* **13**, 797 (1986).

⁹R. L. Stenzel, W. Gekelman, and J. M. Urrutia, *Adv. Space Res.* **6**, 135 (1986).

¹⁰B. U. Ö. Sonnerup, in *Solar System Plasma Physics*, edited by C. F. Kennel, L. J. Lanzerotti, and E. N. Parker (North-Holland, New York, 1979).

¹¹N. J. Fish, *Rev. Mod. Phys.* **59**, 1 (1978).